Thermostability enhancement and change in starch hydrolysis profile of the maltohexaose-forming amylase of *Bacillus stearothermophilus* US100 strain

Mamdouh BEN ALI*, Bassem KHEMAKHEM*, Xavier ROBERT†, Richard HASER† and Samir BEJAR*[1]

*Centre de Biotechnologie de Sfax, BP 'K' 3038 Sfax, Tunisia, and †Laboratoire de BioCristallographie, Institut de Biologie et Chimie des Protéines, UMR 5086-CNRS/Université de Lyon I, IFR128 'BioSciences Lyon-Gerland', 7 Passage du Vercors, F-69367 Lyon Cedex 07, France

The implications of Asn^{315} and Val^{450} in the atypical starch hydrolysis profile of *Bacillus stearothermophilus* Amy (α-amylase) US100 have been suggested previously [Ben Ali, Mhiri, Mezghani and Bejar (2001) Enzyme Microb. Tech. **28**, 537–542]. In order to confirm this hypothesis, three mutants were generated. Of these two have a single mutation, N315D or V450G, whereas the third contains both mutations. Analysis of the starch breakdown-profile of these three mutants, as well as of the wild-type, allowed us to conclude that each single mutation induces a small variation in the hydrolysis product. However, the major end product produced by the double mutant shifts from maltopentaose/maltohexaose to maltose/maltotriose, confirming the involvement of these two residues in starch hydrolysis. The superimposition of AmyUS100 model with that of *Bacillus licheniformis* shows in AmyUS100 an additional loop containing residues Ile^{214} and Gly^{215}. Remarkably, the deletion of these two residues increases the half-life at 100 °C from 15 min to approx. 70 min. Moreover, this engineered amylase requires less calcium, 25 p.p.m. instead of 100 p.p.m., to reach maximal thermostability.

Key words: α-amylase, *Bacillus stearothermophilus*, starch hydrolysis profile, thermostability.

INTRODUCTION

Amys (α-amylases) (1,4-α-D-glucan glucanohydrolase, EC 3.2.1.1) catalyse the hydrolysis of α-(1,4) glycosidic linkages in starch and related polysaccharides. They belong to family 13 in the classification of glycoside hydrolases [1]. This family is the most varied of all glycoside hydrolase families, containing many enzymes able to catalyse various reactions, such as hydrolysis, transglycosylation, condensation and cyclization [2,3].

Among the Amys, the bacterial enzymes are the most diverse as far as physicochemical properties are concerned. These properties include the optimum temperature and pH, and the substrate specificity, as well as the end product of hydrolysis [4]. Some atypical Amys, producing specific malto-oligosaccharides at high yields, have considerable commercial importance. Indeed, the demand for dextrines containing a relatively large quantity of malto-oligosaccharides (such as maltohexaose and maltopentaose) has increased due to their relatively low molecular mass, sweetness and digestibility, as well as their high absorbability [5]. Despite the importance of such atypical Amys, little information is available about the amino acid sequence and three-dimensional structure differences between these enzymes and the typical Amys, which produce maltose and maltotriose as the major end products of starch hydrolysis. Indeed, the structures of only three such enzymes are resolved: the maltohexaose-producing Amy from alkalophilic *Bacillus* sp. 707 [6] and from *Klebsiella pneumoniae* [7], and the maltotetraose-producing Amy from *Pseudomonas stutzeri* [8].

X-ray diffraction studies of a number of Amys have shown that they consist of three domains, called A, B and C [9]. The central $(\beta/\alpha)_8$ barrel (domain A) forms the core of the molecule and contains the three catalytic residues Asp^{231}, Glu^{261} and Asp^{328} (BLA [*Bacillus licheniformis* Amy] numbering). Domains B and C are located at roughly opposite sides of this TIM-barrel.

The study of structure–function relationships, mutagenesis and molecular modelling has allowed the identification of several residues implicated in the physico-chemical properties of Amys and has led to the design of optimally performing enzymes for several applications [4,10]. Hence, Joyet et al. [11] and Declerk et al. [12,13] have shown that the H133I and A209V mutations increase the half-life of BLA 10-fold at 90 °C. Recently, Declerk et al. in [14] reported that the accumulation of five substitutions in BLA (H133I, N190F, A209V, Q264S and N265Y) leads to a drastic increase in thermostability compared with wild-type enzyme or to single mutant enzymes. Igarashi et al. [15] demonstrated that the substitution R124P or the deletion of the Arg^{181} and Gly^{182} residues of AmyK (*Bacillus* sp. strain KSM-K38 Amy) increases thermostability, whether or not $CaCl_2$ was present. They also demonstrated that the mutation of Met^{202} to non-oxidizable residues enhance oxidative stability of the enzyme [15].

We have previously reported the characterization and molecular cloning of a thermostable atypical Amy from the *Bacillus stearothermophilus* US100 strain (AmyUS100) [16]. The purification of the recombinant enzyme, as well as the primary sequence determination and analysis of AmyUS100, were reported [17].

Primary sequence examination of AmyUS100 showed that AmyS (*B. stearothermophilus* strain DN1792 Amy) [18] shares only three different residues in comparison with the mature protein. These substitutions take on more importance when one considers that these two Amys differ only in their starch hydrolysis profile [17]. Among these amino acids, we have hypothesized the implications of Asn^{315} and Val^{450} substitutions [the third

Abbreviations used: Amy, α-amylase; AmyK, *Bacillus* sp. strain KSM-K38 Amy; AmyS, *Bacillus stearothermophilus* strain DN1792 Amy; AmyUS100, *B. stearothermophilus* strain US100 Amy; BAA, *Bacillus amyloliquefaciens* Amy; BLA, *Bacillus licheniformis* Amy; BSTA, *B. stearothermophilus* ATCC12980 Amy; G1, glucose; G2, maltose; G3, maltotriose; G4, maltotetraose; G5, maltopentaose; G6, maltohexaose; G7, maltoheptaose.

[1] To whom correspondence should be addressed (email Samir.bejar@cbs.rnrt.tn).

substitution (Thr^{525}) is located in the terminal part of domain C and is therefore likely to have less functional significance]. Furthermore, the structure comparison of AmyUS100 and BLA showed that the former has two residues forming an extra loop in domain B, which seems to be implicated in thermostability, as suggested by Igarashi et al. [15].

In the present study we investigated the catalytic role for Asn^{315} and Val^{450} in atypical starch hydrolysis, as well as the investigation of the effect of deleting Ile^{214} and Gly^{215} on thermostability and calcium requirements.

EXPERIMENTAL

Media, bacterial strains and plasmids

Media used were Luria broth, Luria agar, Minimal M9 containing 1 % (w/v) soluble starch and ampicillin (100 μg/ml). Bacteria were cultured in 500 ml Erlenmeyer flasks, with agitation at 250 rev./min, at 37 °C.

Escherichia coli DH5α [F^- Φ80 Δ*lac*ZΔM15 Δ(*lac*ZYA-*arg*F) U169 *end*A1 *rec*A1 *hsd*R17 (r_k^-, m_k^+) *deo*R *thi*-1 *sus*E44 λ^- *gyr*A96 *rel*A1] (Invitrogen) was used as the host strain. *E. coli* blueXL1-Blue strain {*rec*A1 *end*A1 *gyr*A96 *thi*-1 *hsd*R17 *sup*E*44* *rel*A1 lac [*F' pro*AB lacI^q Δ*lac*ZΔM15 *Tn10* (*Tet*^{r})]} was supplied with the QuikChange® site-directed mutagenesis kit from Stratagene and was used as the host strain for site-directed mutagenesis. *E. coli* ER2566 {F^- λ^- *fhu*A2[lon] omp T lac Z *::*T7 gene 1 gal sulA11 Δ(mcrC-mrr) 114 *::*IS10 R(mcr-73 *::*miniTn10- TetS)2 R(zgb-210 *::*Tn10) (TetS) endA1 [dcm]} and the pTYB12 intein-fusion expression vector are part of the IMPACT system and were purchased from New England Biolabs. pMBA1 was previously described in [17]. pMBA13, pMBA14, pMBA15, pMBA16 and pMBA17 are plasmids containing intein fused with AmyUS100, AmyUS100-D (containing the mutation N315D), AmyUS100-G (V450G), AmyUS100-D/G (containing the double mutation N315D/V450G) and AmyUS100-ΔIG (Ile^{214} Gly^{215} deletion) respectively. All these plasmids were made by cloning the respective amplified genes into the SmaI site of pTYB12.

Enzyme assays and hydrolysis product analyses

The assay of Amy activity was performed at 80 °C and pH 5.6 for 30 min. The reaction mixture contained 0.5 % (w/v) starch in 25 mM acetate buffer (pH 5.6) and the enzyme solution in a final volume of 1 ml. The amount of enzyme required to produce reducing sugars equivalent to 1 μmol of glucose per minute was defined as one unit of Amy. The concentration of reducing sugar was determined by the DNS (dinitrosalicylic acid) method, described in [19].

End-product analysis was performed using HPLC, on an Aminex HPX-42A saccharide analysis column (Bio-Rad Laboratories), with water as the mobile phase (flow rate 0.3 ml/min) at 85 °C and a differential refractometric detector (10A from Shimadzu). G1 (glucose), G2 (maltose), G3 (maltotriose), G4, (maltotetraose) G5 (maltopentaose), G6 (maltohexaose) and G7 (maltoheptaose) were used as standards and purchased from Sigma–Aldrich.

Purification of recombinant Amys, protein quantification and electrophoresis

Purification of AmyUS100 and derived mutants was performed using the IMPACT-CN system from New England Biolabs. The target protein was fused to a tag consisting of the intein and the chitin-binding domain, which allows affinity purification of the fusion precursor on a chitin column. This kit utilizes the inducible self-cleavage activity of a protein-splicing element (intein) to separate the target protein from the affinity tag. *E. coli* ER2566 cells containing the plasmids (pMBA13–17) were induced to an attenuance of 0.5–0.6 with 0.1 mM isopropyl 1-thio-β-D-galactopyranoside and grown overnight at 23 °C. Cells were harvested by centrifugation, resuspended in 20 mM Tris/HCl (pH 8.0), 500 mM NaCl and 1 mM EDTA, and disrupted by sonication in the presence of a mixture of protease inhibitors (Sigma). Debris was removed by centrifugation at 30 000 ***g*** for 30 min at 4 °C, and then the supernatant was applied to a column containing the IMPACT-NT chitin-resin. Self-cleavage of the intein was carried out by overnight incubation with 50 mM dithiothreitol at 4 °C. Eluted proteins were pure, as judged by SDS/10 % PAGE.

Protein concentration was determined by the Bradford method [20] using BSA as the standard. Enzymes were separated by SDS/10 % PAGE according to the method of Laemmli [21]. Protein bands were visualized by Coomassie Brilliant Blue R-250 (Bio-Rad Laboratories) staining.

DNA isolation, manipulation and mutagenesis

General molecular biological experiments involving plasmid purification, enzyme digestion and modification, and *E. coli* transformation, were performed in accordance with the methods described in Molecular Cloning [22] or Current Protocols in Molecular Biology [23].

Mutations were introduced using the QuikChange® site-directed mutagenesis kit from Stratagene according to the manufacturer's instructions. The primer 5′-CATTACGAAAAC-GACGGAACGATGTCT-3′ was used to construct AmyUS100-D; the primer 5′-ACAAGGGAAGGGGGCACTGAAAAACC-3′ was used to construct AmyUS100-G; and the primer 5′-GCATTT-ACAAATTCCGCGGCAAAGCGTGGGATTG-3′ was used to construct AmyUS100-ΔIG. The presence of the appropriate deletion or substitutions and the absence of unwanted mutations were confirmed by sequencing the inserts.

Computer-aided modelling of the tertiary structure of Amy

The automated protein structure homology-modelling server, SWISS-MODEL [24] (http://www.expasy.org/swissmod/), was used to generate the three-dimensional model. The Deep View Swiss-PDB Viewer software from the EXPASY server (available at http://www.expasy.org/spdbv) was used to visualize and analyse the atomic structure of the model. Molecular modelling of AmyUS100 was analysed based on the X-ray crystallographic structure of BLA (PDB accession code 1BLI) and BSTA (*B. stearothermophilus* ATCC12980 Amy; PDB accession code 1HVX). Finally, VIEWERLITE™ 5.0 (Accelrys, http://www.accelrys.com/) was used to render the structures.

RESULTS AND DISCUSSION

Contribution of the Asn^{315} and Val^{450} residues to the change in starch breakdown products

AmyUS100 is a thermoactive atypical Amy producing maltohexaose and maltopentaose as main end products of starch hydrolysis [16]. Amino acid sequence analysis of AmyUS100 and AmyS [18] showed that they differ by only three residues out of the 516 in the mature protein. These substitutions take on more importance when one considers that these two Amys have approximately the same optimum pH and temperature, but differ in their profiles of starch hydrolysis [17]. Among these

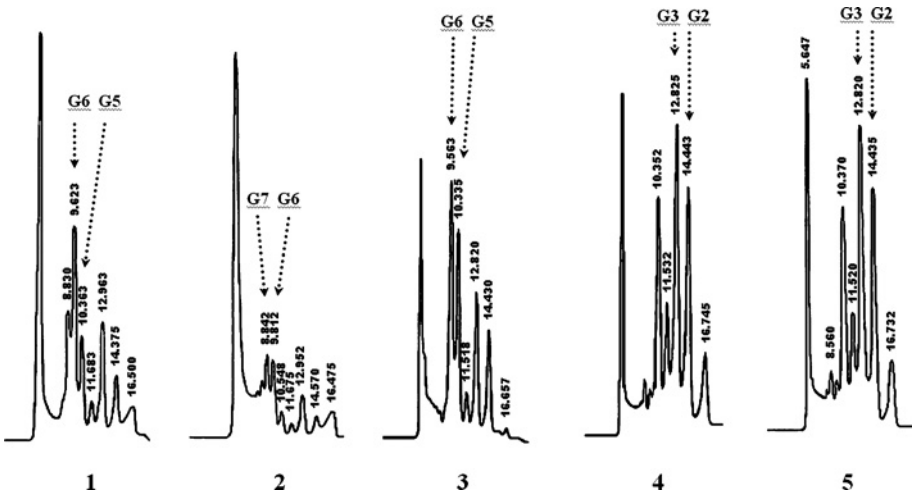

Figure 1 Comparison of the starch hydrolysis profile

The HPLC end product profiles of starch hydrolysis by AmyUS100-G (**1**), AmyUS100-D (**2**), AmyUS100 (**3**), AmyUS100-D/G (**4**) and AmyS (**5**). The reaction was performed at 80 °C and pH 5.6 for 24 h on 1 % (w/v) soluble potato starch using 1500 unit/g. The major oligosaccharides are indicated for each profile.

substituted amino acids we have suspected that Asn^{315} and Val^{450} are responsible for this change, but that Thr^{525} is not involved since it is located in the terminal region of domain C, which is reported not to be involved in catalysis. In order to confirm this hypothesis, we have generated three mutants by site-directed mutagenesis: AmyUS100-D, AmyUS100-G and AmyUS100-D/G. AmyUS100-D, AmyUS100-G and AmyUS100-D/G are AmyUS100 variants harbouring the mutations N315D, V450G and the double mutant N315D/V450G respectively. Subsequently, the different recombinant ER 2566 strains, harbouring the wild-type enzyme and its mutant derivatives, were used for the production and purification of the different Amys. The starch hydrolysis profile of the wild-type and the three mutant enzymes, after 24 h of hydrolysis in the presence of the same enzyme/substrate ratio, is illustrated in Figure 1. The analysis of the starch hydrolysis spectra of these three mutants showed that the V450G mutation did not affect the profile of starch hydrolysis, while the second substitution induces a minor change. However, the introduction of both substitutions strongly affects the hydrolysis profile since the main end products shift from G6/G5 to G3/G2 and become remarkably similar to those observed for AmyS.

Structure–function relationships associated with Asn^{315} and Val^{450} mutations

To investigate the effect of the substitutions at a molecular level, a three-dimensional model of AmyUS100 was constructed, on the basis of the crystal structure of the highly similar (97 % sequence identity) BSTA [25]. The AmyUS100 model shows a perfect superimposition with BSTA as the R.M.S.D. (root mean square deviation) of the spatial location for all Cα is very small (approx. 0.05 Å; 1 Å = 0.1 nm).

In order to determine the subsites of AmyUS100, we have inserted into the model the well known glycosidase inhibitor acarbose as a substrate analogue [26], using a computer aided docking experiment. The analysis of the various interactions between the enzyme and the ligand acarbose, and the comparison of the latter complex with other models especially that of a BAA (*Bacillus amyloliquefaciens* Amy)/BLA chimera [26], suggests that the active site could contain ten subsites. By sequence similarity, we also found two calcium-binding sites already described for BLA [27,28] and for BSTA [29]. The first site contains CaI (calcium ion number I, which is strictly conserved in all Amys) and CaII (the second calcium ion of the first calcium-binding site, located between A and B domain of the A molecule) [29]. These two ions form, together with a sodium ion, a linear triad (Ca^{2+}-Na^{+}-Ca^{2+}) as described in BLA and BSTA, and which may also be present in AmyUS100. The second site [which contains CaIII (the third calcium ion)], contributes to the bridging of domain A and C.

Structural analysis of the AmyUS100 model shows that residue Asn^{315} is located at the end of the Aα4 (helix 4 of the TIM-barrel that forms domain A) pointing its side chain towards the surface of the molecule, whereas Val^{450} is located between β1 and β2 strands of the domain C. It is important to note that these residues are far away from the active site and the mechanism(s) for their involvement in the modification of the starch hydrolysis profile is not straightforward. Comparison between the models of AmyUS100 and its double mutant derivative revealed that no significant structural change is induced by the mutations. Accordingly, the active site structure is conserved and the interactions expected between the enzyme and the substrate, in the different subsites, would be preserved in the mutated enzyme.

A close examination of the AmyUS100 model and its superimposition with the generated model of AmyUS100-D/G did not help to explain the changes of starch hydrolysis profiles. The same conclusion has been reported by Emori et al. [30], on the basis of a comparative study between the Amy of *Bacillus subtilis* IAM1212 and that of *B. subtitlis* 2633. The two Amys differ by only five amino acids but have different hydrolysis products. Further analysis of these Amys, based on chimeric proteins, revealed that only one amino acid substitution is responsible for this variation in hydrolysis products [30]. This residue is located in a loop between Aα5 and Aβ5 and does not have any direct implication in the active site. The structural comparison between the models of these enzymes failed to explain the basis of their catalytic differences. It seems clear that crystal structures at high resolution (instead of computer-generated models) are needed for a better understanding of the role of these residues, and crystallization experiments are underway with AmyUS100 and the appropriate mutants.

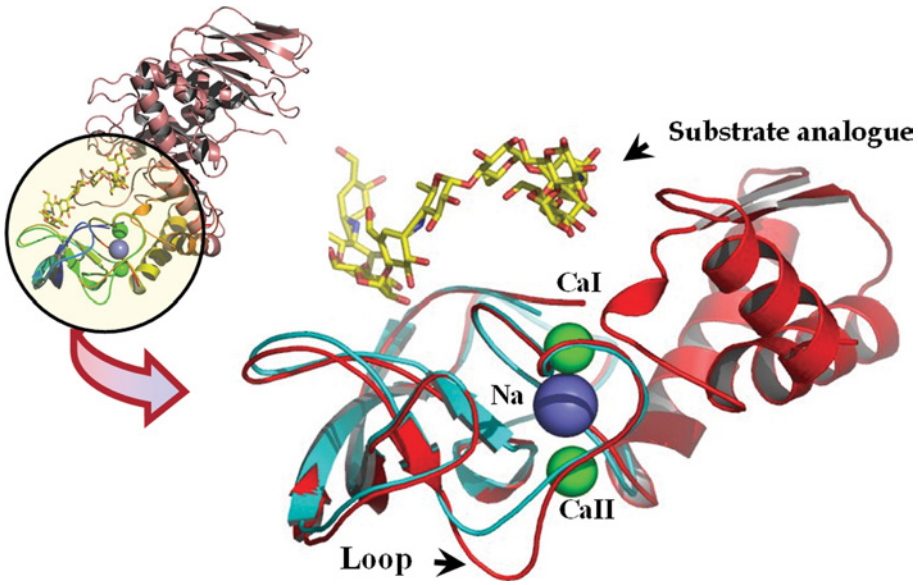

Figure 2 Loop region

The superimposition of AmyUS100 and BLA B domains, focusing on the loop region (Ile^{214} and Gly^{215} using AmyUS100 numbering). AmyUS100 (red); BLA (cyan); calcium ions (green spheres); sodium ion (blue sphere). The substrate analogue (yellow stick) occupies the active site.

Thermostability enhancement of AmyUS100 by deletion of the residues Ile^{214}–Gly^{215}

In order to understand the specificity of the AmyUS100, it was structurally compared with several other Amys including BLA. This comparison revealed the existence, in domain B of AmyUS100, of a small extra loop containing Ile^{214}–Gly^{215} (Figure 2). Following the proposal of Suzuki et al. [31] for other bacterial Amys, we have suspected that this loop is involved in causing the relative low thermostability of AmyUS100 compared with BLA. Indeed, Suzuki et al. in [31] confirmed that the thermostability of BAA was greatly increased by the deletion of the equivalent loop formed by Arg^{176}–Gly^{177} (BAA numbering) and substitution of alanine for Lys^{269}, using site-directed mutagenesis. They suggested that an increase in hydrophobicity, by changing charged residues into non-polar ones, increases the thermostability of this enzyme. Both of these mutations caused a significant and additive thermostabilization of BAA. The Arg^{176}–Gly^{177} deletion has been transferred to a number of other Amys derived from various *Bacillus* species and similar effects on the thermostability were observed [32,33].

Machius et al. [27] also pointed out that the loop containing the Arg^{176}–Gly^{177} residues in BAA has two additional amino acid residues in comparison with BLA, which could cause the increase of flexibility within this region leading to the fall in the thermostability of the whole protein. With the aim of investigating the effect of such a deletion in AmyUS100, we have generated AmyUS100-ΔIG by deleting the Ile^{214}–Gly^{215} residues from the AmyUS100 protein by site-directed mutagenesis.

The study of the thermostability of the mutant exhibits a spectacular effect. Figure 3 shows that the deletion increases the enzyme half-life from 15 min to 70 min at 100 °C, and from 3 min to 13 min at 110 °C, in presence of 100 mM $CaCl_2$.

The involvement of the residues isoleucine and glycine, in similar Amy regions, in thermostability was also suggested by Suvd et al. [29], when studying BSTA. The authors also proposed the involvement of the Ile^{214}–Gly^{215} residues in the stability of the enzyme and, furthermore, do not agree with the claims of Suzuki et al. [31], who implicate the residues Gly^{213}–Ile^{214}. To explain their proposal, Suvd et al. [29] suggested that Ile^{214}–Gly^{215} pushes away a nearby contacting region containing Asp^{207}, which is a

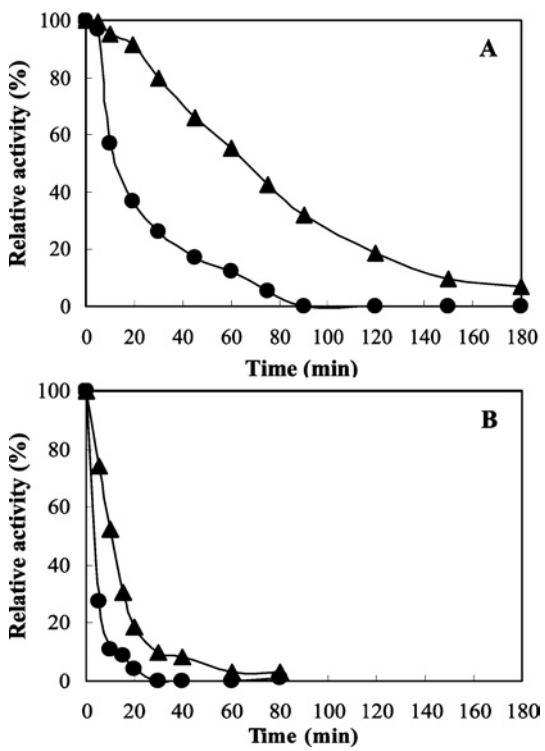

Figure 3 Comparison between the thermostability of AmyUS100 and AmyUS100ΔIG

The residual activity was expressed in terms of the relative activities after incubation at 100 °C (**A**) and 110 °C (**B**), in the presence of 100 p.p.m. of calcium at pH 5.6. (●): AmyUS100; (▲): AmyUS100ΔIG.

calcium ligand. Therefore Asp^{207} can no longer bind to this ion and it is suggested that a water molecule replaces this co-ordination. They suggested that this may be the reason why BSTA, BAA and AmyK are less thermostable than BLA and they hypothesised that the Ile^{214}–Gly^{215} deletion strengthens the enzyme by stabilizing the triad Ca^{2+}-Na^{+}-Ca^{2+}, especially CaII which would be co-ordinated by Asp^{207}, as in BLA. This point has been also discussed by Declerk et al. in [10], when studying the importance of the Ca^{2+}-Na^{+}-Ca^{2+}-binding site at the domain A/B interface of BLA. They have shown the importance of this metal triad for maintaining the proper folding of domain B and the overall conformation of the active site cleft. However, a similar triadic metal-binding site is also present in less thermostable bacterial homologues, as reported for BSTA [25] and for a BAA/BLA chimera [26]. Declerk et al. [10], claim that the enhanced thermostability displayed by BLA could not be attributed to the presence of this metal triad alone. However, in the BSTA structure, the network of interactions around the metal ions is slightly different, since one interaction involving Asp^{207} is missing, and this could partly explain the loss of stability. But in the BAA/BLA chimera, the network of interactions made of by the BAA residues is identical with that seen in BLA.

Decrease in AmyUS100-ΔIG calcium requirements

The structural comparison between the AmyUS100 and the AmyUS100-ΔIG models illustrates the fact that the deletion induces a slight structural rearrangement. The present study also shows that the deletion probably affects the calcium-binding sites. Hence, the model shows that CaII looses interactions with Asp^{105} and His^{238} which contribute to maintainance of the connections between the A and B domains. This observation, in addition to the increase in thermostability, favours a probable decrease in the calcium requirement by AmyUS100-ΔIG. Studies of AmyUS100 and AmyUS100-ΔIG thermostability, in the presence of different concentrations of calcium, confirmed this hypothesis. In fact, the maximal stability of AmyUS100 is obtained with 100 p.p.m. of calcium, while only 25 p.p.m. is needed for AmyUS100-ΔIG (Figure 4).

Our result for AmyUS100 is clearly not consistent with the prediction of Suvd et al. [29], who predicted a Ile^{214}–Gly^{215} deletion stabilizing CaII which would be co-ordinated by Asp^{207}, as in BLA. Indeed, we have shown that this deletion pushes away the spatially contacting region, including Asp^{207} which corresponds to the Ca^{2+}-co-ordinating Asp^{204} in BLA. Thus, and as shown by superimposition of the two models of AmyUS100 and AmyUS100-ΔIG, the orientation of the Asp^{207} side chain was changed to be further away from CaII, avoiding any kind of the co-ordination predicted (Figure 5). Analysis of the AmyUS100 model and its deleted derivative seems to show that the deletion abolishes the interactions between CaI, Asp^{105} and His^{238}, contributing to the maintainance of folding and ther conformation of domain B and the active site cleft. This deletion could also minimize the interactions between the enzyme, CaII and CaIII (results not shown). These indications support the decreased calcium requirements of the deletion mutant of Amy and the increase in thermostability. They also suggest that the CaI site, and to a lesser degree the CaII and CaIII binding sites, are not as necessary for the AmyUS100-ΔIG as compared with the wild-type enzyme. This hypothesis is experimentally strengthened when one considers that the maximal stability of the enzyme is reached at only 25 p.p.m. of calcium for AmyUS100-ΔIG instead of the 100 p.p.m. required by the wild-type. As this increase in the thermostability of the mutant AmyUS100-ΔIG, compared with the wild-type *Bacillus* Amy, occurs in the presence of lower calcium levels, it is not ion-dependent. This result can be explained in term of rigidity enhancement, probably due to the weak interactions generated by the structural rearrangement caused by the deletion. The importance of such interactions was discussed by Feller et al. [34] and Aghajari et al. [35] when studying

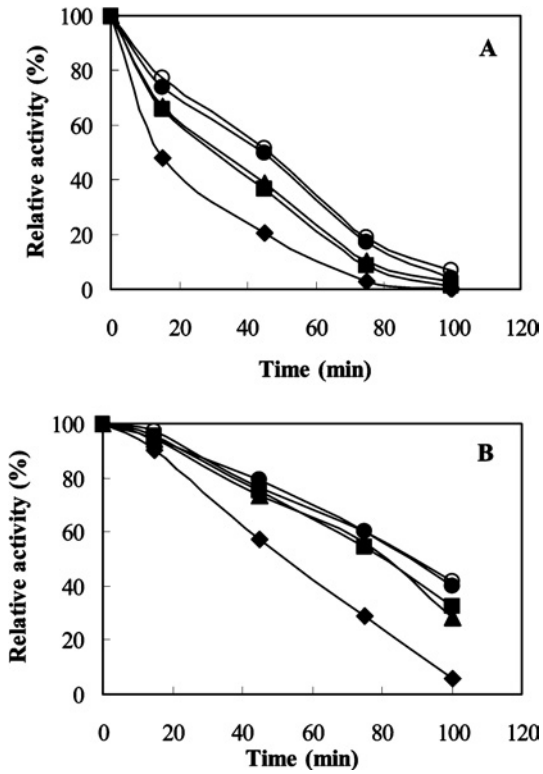

Figure 4 Effects of the loop deletion on the calcium demand

Thermostability comparison of AmyUS100 (**A**) and AmyUS100-ΔIG (**B**) at 100 °C and pH 5.6 in presence of different calcium concentrations (◆): 0 p.p.m.; (■): 25 p.p.m.; (▲): 50 p.p.m.; (●): 100 p.p.m.; (○): 200 p.p.m.

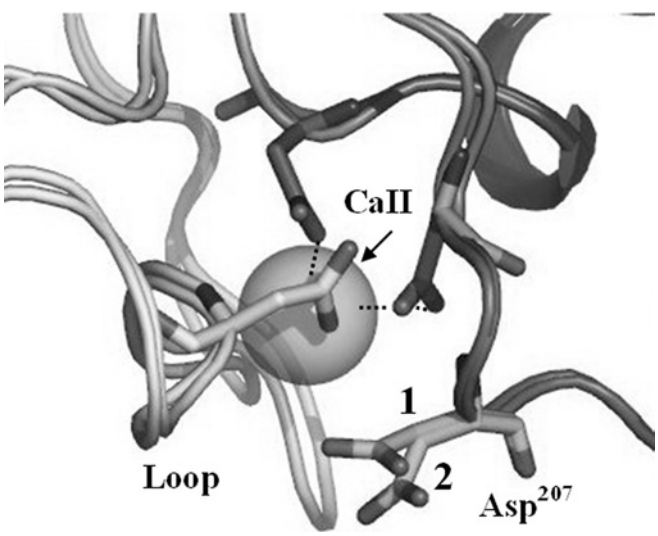

Figure 5 Network of interactions around CaII

Superimposition of US100 and Amy US100-ΔIG, focusing on the CaII region, showing the position and side-chain orientation of Asp^{207} in Amy US100 (**1**) and in Amy US100-ΔIG (**2**). Broken lines, hydrogen bonds.

cold adaptation and stability in the psychrophilic Amy from *Pseudoalteromonas haloplanktis*. These studies were confirmed and extended by D'Amico et al. [36] who suggested that the psychrophilic Amy has lost numerous weak interactions during evolution to reach the proper conformational flexibility at low temperatures. These adaptive adjustments contribute to improve the k_{cat} without alterating the catalytic mechanism as the active site architecture is not modified, but at the expense of a weaker substrate binding affinity. On the other hand, thermophilic enzymes strengthen the same type of interaction to gain in structural stability at high temperatures, but do so at the expense of a poor activity at low temperature.

The new characteristics of the engineered AmyUS100 appear to be crucial in terms of potential industrial applications, since these will contribute to a significant decrease in the process cost. AmyUS100-ΔIG will have great commercial value, since it is the most thermostable Amy producing maltohexaose and has low calcium requirements.

This research was supported by the Tunisian government Contract Programme CBS-LEMP (Centre de Biotechnologie de Sfax-Laboratoire d'Enzymes et Métabolites des Procaryotes), the ICGEB [International Centre of Genetic Engineering and Biotechnology; CRP/TUN (Collaborative Research Project) 00–02] and by the Franco-Tunisian CMCU (Comité Mixte de Coopération Universitaire; N°04/0905).

REFERENCES

1 Davies, G. and Henrissat, B. (1995) Structures and mechanisms of glycosyl hydrolases. Structure **3**, 853–859
2 Svensson, B., Tovborg Jensen, M., Mori, H., Sass Bak-Jensen, K., Bønsager, B., Nielsen, P. K., Birte Kramhøft, B., Prætorius-Ibba, M., Nøhr, J., Juge, N. et al. (2002) Fascinating facets of function and structure of amylolytic enzymes of glycoside hydrolase family 13. Biologia (Bratislava) **57** (Suppl. 11), 5–19
3 Janecek, S. (2002) How many conserved sequence regions are there in the α-amylase family? Biologia (Bratislava) **57** (Suppl. 11), 29–41
4 Nielsen, J. E. and Borchert, T. V. (2000) Protein engineering of bacterial α-amylases. Biochim. Biophys. Acta. **1543**, 253–274
5 Marchal, L. M., Beeftink, H. H. and Tramper, J. (1999) Towards a rational design of commercial maltodextrins. Trends Food Sci. Tech. **10**, 345–355
6 Kanai, R., Haga, K., Akiba, T., Yamane, K. and Harata, K. (2004) Biochemical and crystallographic analyses of maltohexaose-producing amylase from alkalophilic *Bacillus* sp. 707. Biochemistry **44**, 14047–14056
7 Momma, M. and Fujimoto, Z. (2004) Expression, crystallization and preliminary X-ray crystallographic studies of *Klebsiella pneumoniae* maltohexaose-producing α-amylase. Acta Crystallogr. Sect. D Biol. Crystallogr. **60**, 2352–2354
8 Mezaki, Y., Katsuya, Y., Kubota, M. and Matsuura, Y. (2001) Crystallization and structural analysis of intact maltotetraose-forming exo-amylase from *Pseudomonas stutzeri*. Biosci. Biotechnol. Biochem. **1**, 222–225
9 Buisson, G., Duee, E., Haser, R. and Payan, F. (1987) Three dimensional structure of porcine pancreatic α-amylase at 2.9Å resolution. Role of calcium in structure and activity. EMBO J. **6**, 3909–3916
10 Declerck, N., Machius, M., Joyet, P., Wiegand, G., Huber, R. and Gaillardin, C. (2002) Engineering the thermostability of *Bacillus licheniformis* α-amylase. Biologia (Bratislava) **57** (Suppl. 11), 203–211
11 Joyet, P., Declerck, N. and Gaillardin, C. (1992) Hyperthermostable variants of a highly thermostable α-amylase. Biotechnology **10**, 1579–1583
12 Declerck, N., Joyet, P., Trosset, J. Y., Garnier, J. and Gaillardin, C. (1995) Hyperthermostable mutants of *Bacillus licheniformis* α-amylase: multiple amino acid replacements and molecular modelling. Protein Eng. **8**, 1029–1037
13 Declerck, N., Machius, M., Chambert, R., Wiegand, G., Huber, R. and Gaillardin, C. (1997) Hyperthermostable mutants of *Bacillus licheniformis* α-amylase: thermodynamic studies and structural interpretation. Protein Eng. **10**, 541–549
14 Declerck, N., Machius, M., Joyet, P., Wiegand, G., Huber, R. and Gaillardin, C. (2003) Hyperthermostabilization of *Bacillus licheniformis* α-amylase and modulation of its stability over a 50°C temperature range. Protein Eng. **16**, 287–293
15 Igarashi, K., Hagihara, H. and Ito, S. (2003) Protein engineering of detergent α-amylases. Trends Glycosci. Glycotechnol. **82**, 101–114
16 Ben Ali, M., Mezghani, M. and Bejar, S. (1999) A thermostable maltohexaose producing amylase from a new isolated *B. stearothermophilus*: study of activity and molecular cloning of the corresponding gene. Enzyme Microb. Tech. **24**, 584–589
17 Ben Ali, M., Mhiri, S., Mezghani, M. and Bejar, S. (2001) Purification and sequence analysis of the atypical maltohexaose-forming α-amylase of the *B. stearothermophilus* US100. Enzyme Microb. Technol. **28**, 537–542
18 Jørgensen, P. L., Poulsen, G. B. and Diderichsen, B. (1991) Cloning of a chromosomal α-amylase gene from *Bacillus stearothermophilus*. FEMS Microbiol. Lett. **77**, 271–275
19 Miller, G. L. (1959) Use of dinitrosalicylic acid reagent for determination of reducing sugars. Anal. Chem. **31**, 426–428
20 Bradford, M. M. (1976) A rapid and sensitive method for the quantitation of microgram quantities of protein utilizing the principle of protein-dye binding. Anal. Biochem. **72**, 248–254
21 Laemmli, U. K. (1970) Cleavage of structural proteins during the assembly of the head of bacteriophage T_4. Nature (London) **227**, 680–685
22 Sambrook, J., Fritsch, E. F. and Maniatis, T. (1989) Molecular Cloning: A Laboratory Manual, Cold Spring Harbor Laboratory, Cold Spring Harbor
23 Ausubel, F. M., Brent, R., Kingston, R. E., Moore, D. D., Seidman, J. G., Smith, J. A. and Struhl, K. (1993) Current Protocols in Molecular Biology, Greene Publishing Associates and Wiley, New York
24 Schwede, T., Kopp, J., Guex, N. and Peitsch, M. C. (2003) SWISS-MODEL: an automated protein homology-modelling server. Nucleic Acids Res. **31**, 3381–3385
25 Suvd, D., Takase, K., Fujimoto, Z., Matsumura, M. and Mizuno, H. (2000) Purification, crystallization and preliminary X-ray crystallographic study of α-amylase from *Bacillus stearothermophilus*. Acta Crystallogr. Sect. D Biol. Crystallogr. **56**, 200–202
26 Brzozowski, A. M., Lawson, D. M., Turkenburg, J. P., Bisgaard-Frantzen, H., Svendsen, A., Borchert, T. V., Dauter, Z., Wilson, K. S. and Davies, G. J. (2000) Structural analysis of a chimeric bacterial α-amylase. Biochemistry **39**, 9099–9107
27 Machius, M., Wiegand, G. and Huber, R. (1995) Crystal structure of calcium-depleted *Bacillus licheniformis* α-amylase at 2.2 Å resolution. J. Mol. Biol. **246**, 545–559
28 Machius, M., Declerck, N., Huber, R. and Wiegand, G. (1998) Activation of *Bacillus licheniformis* α-amylase through a disorder → order transition of the substrate-binding site mediated by a calcium-sodium-calcium metal triad. Structure **6**, 281–292
29 Suvd, D., Fujimoto, Z., Takase, K., Matsumura, M. and Mizuno, H. (2001) Crystal structure of *Bacillus stearothermophilus* α-amylase: possible factors determining the thermostability. J. Biochem. (Tokyo) **129**, 461–468
30 Emori, M., Takagi, M., Maruo, B. and Yano, K. (1990) Molecular cloning, nucleotide sequencing, and expression of the *Bacillus subtilis* (natto) IAM1212 α-amylase gene, which encodes an α-amylase structurally similar to but enzymatically distinct from that of *B. subtilis* 2633. J. Bacteriol. **172**, 4901–4908
31 Suzuki, Y., Ito, N., Yuuki, T., Yamagata, H. and Udaka, S. (1989) Amino acid residues stabilizing a *Bacillus* α-amylase against irreversible thermoinactivation. J. Biol. Chem. **264**, 18933–18938
32 Igarashi, K., Hatada, Y., Ikawa, K., Araki, H., Ozawa, T., Kobayashi, T., Ozaki, K. and Ito, S. (1998) Improved thermostability of an arginine-glycine residue is caused by enhanced calcium binding. Biochem. Biophys. Res. Commun. **248**, 372–377
33 Bisgaard-Frantzen, H., Svendsen, A., Norman, B., Pedersen, S., Kjærulff, S., Outtrup, H. and Borchert, T. V. (1999) Development of industrially important α-amylases. J. Appl. Glycosci. **46**, 199–206
34 Feller, G., Payan, F., Theys, F., Qian, M., Haser, R. and Gerday, C. (1994) Stability and structural analysis of α-amylase from the antarctic psychrophile *Alteromonas haloplanctis* A23. Eur. J. Biochem. **222**, 441–447
35 Aghajari, N., Feller, G., Gerday, C. and Haser, R. (1998) Structures of the psychrophilic *Alteromonas haloplanctis* α-amylase give sights into cold adaptation at a molecular level. Structure **6**, 1503–1516
36 D'Amico, S., Gerday, C. and Feller, G. (2002) Structural determinants of cold adaptation and stability in a psychrophilic α-amylase. Biologia (Bratislava) **57** (Suppl. 11), 211–219

Received 3 May 2005/28 September 2005; accepted 30 September 2005
Published as BJ Immediate Publication 30 September 2005, doi:10.1042/BJ20050726